Icarus 264 (2016) 213–219

Contents lists available at ScienceDirect

Icarus

journal homepage: www.journals.elsevier.com/icarus

Enhanced erosion rates on Mars during Amazonian glaciation

Joseph S. Levy [a,*], Caleb I. Fassett [b], James W. Head [c]

[a] University of Texas Institute for Geophysics, Austin, TX 78758, USA
[b] Mount Holyoke College, South Hadley, MA 01075, USA
[c] Brown University, Providence, RI 02906, USA

ARTICLE INFO

Article history:
Received 27 May 2015
Revised 23 September 2015
Accepted 23 September 2015
Available online 9 October 2015

Keyword:
Mars, surface
Mars, climate
Geological processes

ABSTRACT

Observations of Mars from the surface and from orbit suggest that erosion rates over the last ~3 Gyr (the Amazonian) have been as slow as 10^{-5} m/Myr and have been dominated by aeolian processes, while ancient (Noachian) erosion rates may have been orders of magnitude higher due to impact bombardment and fluvial activity. Amazonian-aged glacial deposits are widespread on Mars, but rates of erosion responsible for contributing debris to these remnant glacial deposits have not been constrained. Here, we calculate erosion rates during Amazonian glaciations using a catalog of mid-latitude glacial landforms coupled with observational and theoretical constraints on the duration of glaciation. These calculations suggest that erosion rates for scarps that contributed debris to glacial landforms are 4–7 orders of magnitude higher than average Amazonian rates in non-glaciated, low-slope regions. These erosion rates are similar to terrestrial cold-based glacier erosion and entrainment rates, consistent with cold-based glacier modification of parts of Mars.

1. Introduction

The surface of Mars contains crustal units and surface deposits that range in age from >4 billion years to less than a few hundred thousand years (Tanaka et al., 2014). Accordingly, erosion rates estimated for Mars are highly variable as a function of location and the window of time over which erosion occurs (Golombek and Bridges, 2000; Golombek et al., in press). Observations of aeolian deflation at the Pathfinder landing site suggested erosion rates over 1.8–3.5 Gyr of $1–4 \times 10^{-5}$ m/Myr (Golombek and Bridges, 2000). Measurements of crater degradation along the traverse of the Opportunity rover suggest that erosion rates may be up to 1 m/Myr for the freshest craters (0.1–1 Myr), but fall off to <0.1 m/Myr for 10–20 Myr old craters, before decreasing to the slower average rates for craters from the middle to early Amazonian (Golombek et al., in press). Recent measurements of landslide-driven scarp retreat in the interior layered deposits (ILD) of Valles Marineris suggest rapid erosion of these friable, potentially ice-rich, and steeply sloped deposits, on the order of 1.2–2.3 m/Myr over the past 400 Myr (Grindrod and Warner, 2014). In contrast, orbital observations of large, Noachian and Hesperian craters suggest erosion rates in the distant past may have reached up to 1–100 m/Myr (Carr, 1996; Craddock and Maxwell, 1993; Craddock et al., 1997). Here, we calculate erosion rates from debris-bearing glacial landforms that are distributed widely across the martian mid-latitudes and that formed over an extended period of time during the Amazonian.

Erosion associated with cold-based glaciation on Earth is known to be very different and to have much lower rates than wet-based glacial erosion (Hallet et al., 1996). Erosion and sediment formation in wet-based glacial environments occurs primarily due to (1) basal melting, rapid glacial movement, and associated abrasion and transport, as well as (2) freeze–thaw cycling of adjacent outcrops that promotes generation of supraglacial debris. In cold-based glaciation, glacial movement is extremely slow, deformation occurs overwhelmingly within the ice, and generation of meltwater is limited to thin films. These factors combine to result in extremely low basal erosion rates (~9×10^{-1} to 3×10^{0} m/Myr) (Cuffey et al., 2000). Extremely low surface temperatures (thermal cycling but little to no freeze–thaw activity) mean that debris shed from adjacent, steep-walled outcrops is also correspondingly less in environments where cold-based glacial activity dominates than in the case of wet-based glaciers, e.g., Mackay et al. (2014).

For example, the vast majority of debris in and on cold-based glaciers in Antarctica is derived from rockfall and erosion from the steep cliffs that surround the accumulation zones of these glaciers. It is deposited supraglacially, and often becomes englacial by the continued deposition of snow and ice in the accumulation zone. It is returned to the surface debris blanket via glacier flow

* Corresponding author.
E-mail address: joe.levy@utexas.edu (J.S. Levy).

http://dx.doi.org/10.1016/j.icarus.2015.09.037
0019-1035/

and sublimation (Marchant et al., 2002; Marchant and Head, 2007; Mackay et al., 2014). These Antarctic Dry Valley cold-based glaciers are generally protective rather than erosional at their bases (e.g., Denton et al., 1993), although minor basal entrainment of silt and fine sand occur (Cuffey et al., 2000).

Debris-covered glacial deposits on Mars (Figs. 1 and 2), including lineated valley fill (LVF), lobate debris aprons (LDA), and concentric crater fill (CCF), cover 7×10^5 km^2 of the martian surface between ±~30–50° latitude to a thickness of several hundred meters (Levy et al., 2014). LDA, LVF, and CCF are exceptionally common along the martian dichotomy boundary (e.g., the valley-and-mesa fretted terrain in Deuteronilus and Protonilus mensae, Sharp, 1973) and east of the Hellas impact basin (Squyres, 1978). Initial geomorphic analyses of these features interpreted them as indicators of ground ice emplaced by vapor diffusion in a different climate epoch, and the mobilization and flow of ice-cemented debris (boulders and finer-grained sediments) eroded from the escarpments (Sharp, 1973; Squyres, 1978, 1979; Squyres and Carr, 1986). Other studies (Lucchitta, 1984; Head et al., 2006a, 2006b, 2010; Holt et al., 2008; Plaut et al., 2009; Levy et al., 2010; Karlsson et al., 2015) have noted the similarities between these features and terrestrial debris-covered glaciers, both in terms of morphology and radar properties, and have interpreted these features as deposits formed by the accumulation and flow of glacial ice (Li et al., 2005) that are covered by a debris lag derived from erosion and entrainment of debris from the accumulation zone of the glacier.

Morphological criteria use to recognize martian debris-covered glaciers including LVF, LDA, and CCF, include: (1) the presence of alcoves in mesas, valley walls, or crater walls that could have served as ice accumulation zones; (2) parallel or arcuate ridges emerging from these alcoves that are interpreted as flow-derived lineations; (3) tightening or folding of ridges where flow was confined by obstacles such as bedrock ridges; (4) broadening or expansion of lineations in unconfined regions; (5) merging of lineations where two features meet; (6) arête-like morphology of rock spurs between glacial features; (7) merging of LVF, LDA, and/or CCF to form integrated valley glacier systems; and (8) convex-up topography with a parabolic down-slope profile (Head et al., 2010). Radar observations interpreted to indicate a debris-covered glacier origin include (1) radar velocity determinations consistent with water ice

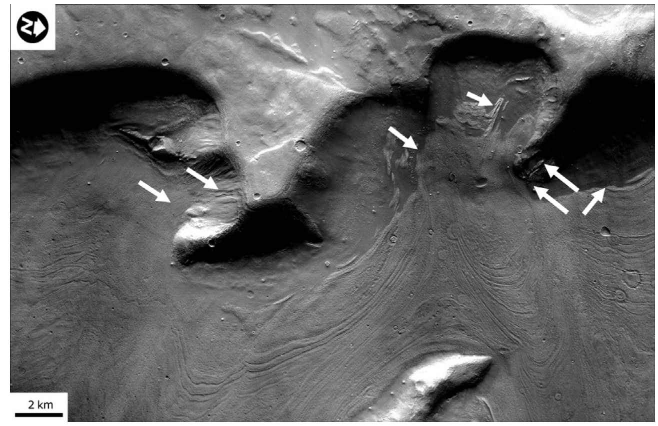

Fig. 2. Example of LDA emanating from sheltered alcoves along a massif. Note that debris-bearing flow lineations (arrows) can be mapped back to glacier accumulation areas in these alcoves, as noted by Head et al. (2006b), implying erosion of sediment in the accumulation zone and transport of the debris down-slope by glacier flow. Portion of CTX image P18_008019_2227.

and (2) a lack of internal reflectors including layers or point reflectors, which is interpreted to indicate clean (low debris content) ice (Holt et al., 2008; Plaut et al., 2009). Lineated debris bands on LDA, LVF, and CCF surfaces extend from the steep scarps bounding their accumulation zones to the termini of these features. This is evidence that headwall material in and around the glacial accumulation zone has been eroded and transported downslope by glacial flow in a process analogous to that observed on Earth (Head et al., 2006b; Fastook et al., 2014) (Fig. 2).

Based on the rarity of glacial outwash (Fassett et al., 2010) or melt features (e.g., kettles, push moraines), LDA, LVF, and CCF have been interpreted as evidence of cold-based glaciation (Head et al., 2010), with glacier ice preserved by a thin debris cover similar to the protective lag that overlies cold-based debris-covered glaciers in Antarctica (Marchant et al., 2002; Marchant and Head, 2007; Fastook et al., 2014; Mackay et al., 2014).

Early workers noted that the rocky debris transported by LVF, LDA, and CCF likely was sourced by erosion from the valley walls, isolated massifs, and craters in and around which the deposits

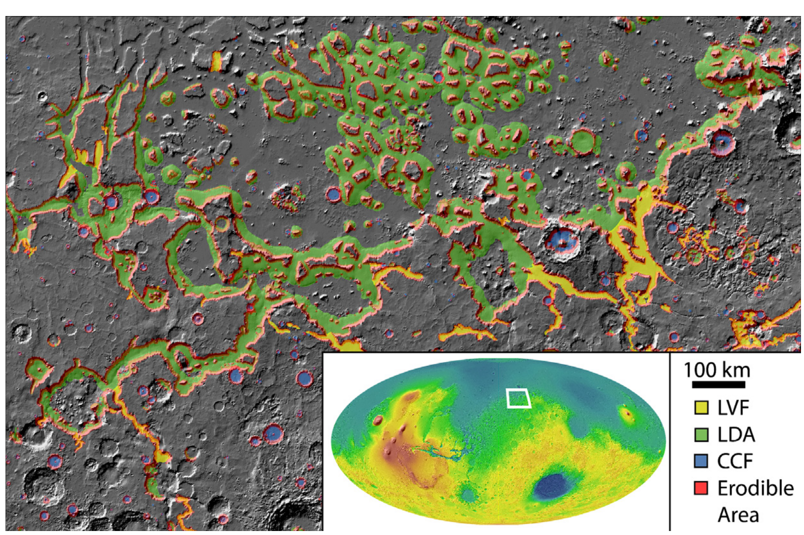

Fig. 1. Map showing the distribution of lineated valley fill (LVF), lobate debris aprons (LDA), and concentric crater fill (CCF) along an example portion of the martian dichotomy boundary (see location inset). The erodible contributing area that could have acted as a source for debris cover sediment based on our contributing area defining method is marked in red. Base map is MOLA 128 ppd gridded topography rendered as a hillshade centered on 41.5°N, 26.5°E. Inset location map is global MOLA 128 ppd topography rendered in hillshade and color-coded elevation (red = high, blue = low) in a Mollweide projection centered on 0°N, 0°E. (For interpretation of the references to color in this figure legend, the reader is referred to the web version of this article.)